JOURNAL OF GEOPHYSICAL RESEARCH, VOL. 112, D21301, doi:10.1029/2007JD008708, 2007

New methodology applied to deriving total ozone and other atmospheric variables from global irradiance spectra

James B. Kerr[1] and John M. Davis[2]

Received 27 March 2007; revised 28 June 2007; accepted 23 July 2007; published 2 November 2007.

[1] A new sampling and analysis method for acquiring low-noise spectra using the Brewer spectrophotometer is applied to ground-based spectral measurements of global ultraviolet radiation. The new technique substantially reduces noise caused by changing atmospheric conditions that can occur during the sampling period. Routine measurements made at Toronto between 1996 and 2006 were used to develop a statistical model for determining total ozone and other variables from the global spectral data. Long-term comparison of global measurements with direct measurements demonstrates that global scan data can be used to measure total ozone with an accuracy better than ±1% for a wide variety of total ozone amounts and vertical profiles under clear skies. Other information such as ozone temperature and instrument wavelength stability can also be extracted. The measurements compared with model results show good agreement for clear-sky conditions. The results indicate that atmospheric aerosols and clouds can enhance absorption of UV radiation by ozone. For aerosol optical depth of one, the absorption enhancement is about 2.0% at air mass value of 1 and drops to 0.5% enhancement for air mass values between 2 and 3. For clouds the enhancement is generally small in winter months but can be substantial in summer months. The statistical relationship used for measuring total ozone using spectral global irradiance data is given. Comparisons of total ozone and ozone temperature derived from global scans with those from direct Sun scans are shown, and the effects of aerosols and clouds on derived total ozone from global data are discussed.

Citation: Kerr, J. B., and J. M. Davis (2007), New methodology applied to deriving total ozone and other atmospheric variables from global irradiance spectra, *J. Geophys. Res.*, *112*, D21301, doi:10.1029/2007JD008708.

1. Introduction

[2] Atmospheric ozone absorbs solar radiation at ultraviolet (UV) wavelengths and in the UV-B (280–315 nm) the absorption increases significantly with decreasing wavelength. The sharp gradient of UV-B radiation reaching the Earth's surface has been used to quantify the amount of ozone in the atmosphere by differential absorption techniques. Several instruments have been developed that sample radiation at selected wavelengths in the UV-B. Ground-based direct Sun measurements of column ozone have been made routinely by Dobson instruments [*Dobson*, 1957], Brewer instruments [*Kerr et al.*, 1981], filter instruments used mainly in the former USSR [*Gustin et al.*, 1985], and, more recently, the U.S. Department of Agriculture UV multifilter rotating shadow-band radiometer (UV-MFRSR) [*Gao et al.*, 2001]. Long-term records from networks of these ground-based instruments have been used to establish global ozone climatology and long-term changes [*World Meteorological Organization*, 2007]. Differential absorption techniques using UV radiation at selected wavelengths are also used to measure atmospheric ozone with satellite instruments such as the Total Ozone Mapping Spectrometer (TOMS), Solar Backscatter Ultraviolet (SBUV), and the Ozone Monitoring Instrument (OMI).

[3] Instruments have been developed to measure atmospheric variables and surface UV irradiance by sampling over wavelength ranges in the UV and visible regions of the solar spectrum. These instruments include single detector spectrometers that sample at different wavelengths sequentially using a mechanical scanning mechanism [*McKenzie et al.*, 1991; *Kerr and McElroy*, 1993; *Booth et al.*, 1994; *Seckmeyer et al.*, 1996; *Harrison et al.*, 2002], as well as relatively new multidetector array spectrometers that sample wavelengths simultaneously [*McElroy*, 1995; *Kiedron et al.*, 2001]. Multifilter instruments are also used to sample UV irradiance at specific wavelengths simultaneously [*Bigelow and Slusser*, 2000; *Høiskar et al.*, 2003]. A summary of the different types of ground-based instruments used for measuring surface UV-B irradiance and atmospheric ozone is presented by *Kerr* [2005].

[4] The most accurately defined method to measure the total column amount of an atmospheric gas is the direct Sun method, where solar radiation passes through the absorbing gas along the direct path. The accuracy of direct Sun total

[1]Environment Canada, Cowichan Bay, British Columbia, Canada.
[2]Ultraviolet Radiation Monitoring and Research Program, U.S. Department of Agriculture, Colorado State University, Fort Collins, Colorado, USA.

0148-0227/07/2007JD008708$09.00

ozone measurements for a well-maintained operational Brewer or Dobson instrument is better than 2% [*Fioletov et al.*, 2005]. Methods have also been developed for determining total ozone by using measurements of global irradiance made with multifilter instruments compared with model results [*Dahlback*, 1996]. An advantage of this technique is that there is no instrumental pointing requirement to select direct radiation. Also, measurements can be made under moderated cloud cover when the Sun is obscured.

[5] One source of error for measurements involving the sampling of wavelength by a mechanical scanning technique is the variability of atmospheric conditions. Scanning over a suitable wavelength range (of ~20 to 100 nm) requires time of up to about 5 minutes for some instruments and during the course of a scan, atmospheric conditions (e.g., clouds or aerosols) are subject to change. The array instruments and multifilter instruments avoid this problem by sampling all wavelengths essentially simultaneously.

[6] The absorption spectra of ozone and other atmospheric trace gases (e.g., sulphur dioxide and nitrogen dioxide) are structured and the absorption features of this structure can be seen if full spectra are taken. This allows for identification of a particular absorber by its unique signature of absorption features and it allows the ability to distinguish between and quantify different absorbing gases (e.g., ozone and sulphur dioxide) that absorb radiation in the same spectral region.

[7] The group-scan method [*Kerr*, 2002] for measuring atmospheric variables is a modified differential absorption spectroscopy (DOAS) technique developed specifically for the Brewer instrument. The Brewer instrument operationally measures radiation at 5 wavelengths spaced by about 3.5 nm that are sampled for about 30 seconds in rapid sequence. Normally, any changes in clouds or aerosols during the measurement interval affect all wavelengths equally because of the rapid and repetitive sampling. The group-scan method mechanically adjusts the five-wavelength group in steps of 0.5 nm at 8 additional settings between the normal operational wavelengths, thereby yielding a full spectral scan of 45 elements. A group scan takes about 3 minutes and the analysis allows uniform scaling between the nine groups of five wavelengths to account for atmospheric fluctuations that may occur between the individual samples.

[8] Since 1996 the group-scan measurements have been made routinely at Toronto. A measurement set includes a global scan, a direct scan and a zenith sky scan made sequentially about 10 to 20 times per day, depending on season. The primary focus of this study is the comparison between global group scans with the adjacent direct scans made 3 minutes later. The global/direct scanning sequence takes about 6 minutes: 3 minutes for each type, and changing atmospheric conditions during the 3-minute scan periods are minimized.

[9] Full details of the direct Sun group-scan sampling technique including wavelength settings and resolution, instrumental calibration and characterization, data analysis technique, and uncertainty estimates are given by *Kerr* [2002]. The previous paper demonstrated that the group-scan method reduces effects of variable atmospheric conditions during the 3-minute sample period of a group scan and that scan data yield measurements of total ozone, effective ozone temperature, atmospheric SO_2, aerosol optical depth, and an atmospheric variability parameter. The present paper reports results of the group-scan method applied to measurements of global radiation with the goal of application of the results to other instrument types.

2. Group Scan Applied to Global Irradiance

[10] The group scans for global irradiance use the same wavelengths and sampling technique as the direct Sun scans [*Kerr*, 2002]. Instrumental corrections (dead time, dark count, neutral density filters, temperature dependence, and stray light) are identical for both global and direct irradiance and these corrections are applied to global data using the same methods as the corrections to direct data. Also, the calibration information used for the global group-scan analysis is the same as that used for the direct analysis. Calibration information includes the extraterrestrial (ET) spectrum, the local slope and curvature of the ET spectrum, ozone absorption coefficients [*Bass and Paur*, 1985], correction for nonlinear ozone absorption resulting from strong gradients of the ozone absorption across the slit passbands [*Vanier and Wardle*, 1969; *Gröbner and Kerr*, 2001], temperature dependence of ozone absorption, and SO_2 absorption coefficients. Determination of these instrumental-dependent calibration data is presented in detail by *Kerr* [2002].

[11] Analysis of the direct group-scan spectra is done by an iterative least squares fitting procedure using the following set of 45 equations (i = 1 to 45) that was given as equation (3) by *Kerr* [2002]:

$$\log(I_{oi}/I_i) - \beta_i m = A_g + B\frac{(\lambda_i - 315\ \text{nm})}{315\ \text{nm}} + C\frac{\Delta\log(I_{oi})}{\Delta ms} + D\alpha_i + E\frac{\Delta\alpha_i}{\Delta T} + F\alpha'_i + \varepsilon_i, \quad (1)$$

where I_{oi} is the ET irradiance at wavelength λ_i; I_i is the measured irradiance at λ_i; β_i is the Rayleigh scattering coefficient at λ_i; g is the group number between 1 and 9; A_g are 9 offset values (one for each group); B is a linear wavelength-dependent term; C is the wavelength offset between the reference scan ($\log(I_{oi})$) and the measured scan ($\log(I_i)$) denoted in micrometer steps (ms); $\Delta\log(I_{oi})/\Delta ms$ is the local slope of the ET irradiance at λ_i with respect to ms; D is the ozone amount seen in the path (= total ozone (X) times air mass path length (μ)); α_i is the ozone absorption coefficient at λ_i at $-45°C$; E is the amount of ozone in the path times the temperature departure from $-45°C$; $\Delta\alpha_i/\Delta T$ is the ozone temperature dependence values at λ_i at $-45°C$; F is the amount of SO_2 seen in the path; α'_i is the SO_2 absorption coefficient at λ_i; and ε_i is the residual value at λ_i. Further detailed descriptions of the iterative analysis technique and interpretation are given by *Kerr* [2002].

[12] The analysis technique for global irradiance differs from that for direct Sun since the infilling of spectra must be considered owing to molecular scattering. This infilling, commonly called the Ring effect [*Grainger and Ring*, 1962], has been observed by several researchers who measure atmospheric constituents using ultraviolet/visible zenith sky spectra and is due to Raman scattering by air

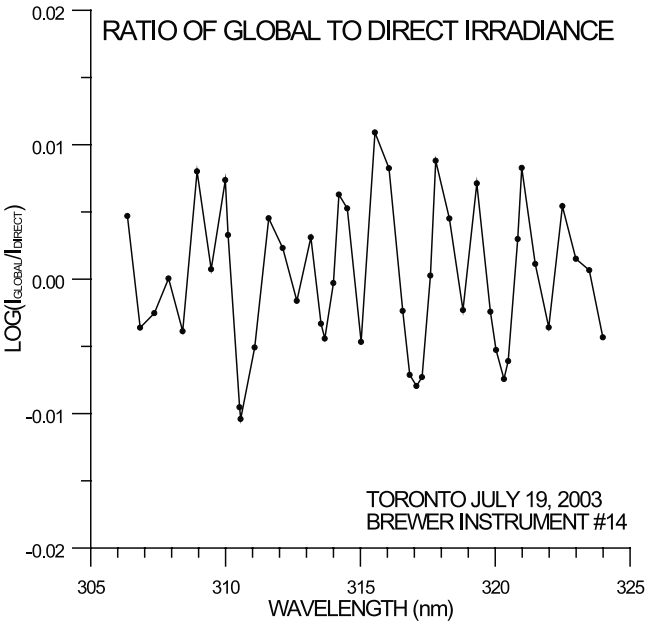

Figure 1. The average ratio of 12 near-simultaneous global/direct spectra made on 19 July 2003 at solar zenith angles ranging between 23° and 55°. Peak values in the ratio spectrum match minimum values, implying that global irradiance is relatively higher at solar minima. The fluctuations seen at this resolution represent about a 4% infilling. This vector is used as an independent variable (ρ in equation (2)) for the global group-scan analysis.

[e.g., *Langford et al.*, 2007]. The Ring effect is illustrated in Figure 1. Here the log of the ratio of global to direct irradiance is shown for the 45 wavelength settings used in the group-scan method. The measurements shown in Figure 1 are the average of 12 near simultaneous (within 3 min) global-direct scan sets made under clear-sky conditions at Toronto on 19 July 2003. The range of solar zenith angles for the 12 scan pairs was between 23° and 55°. The effects of ozone absorption, an offset common to all wavelengths, and linear wavelength dependence were removed. Peak values shown in Figure 1 match minimum values in the solar spectrum (i.e., global irradiance is relatively large for minima in the solar spectra) and the variations represent about a 4% infilling of the direct solar spectrum. For the global analysis, the vector shown in Figure 1 is used as an additional independent variable to account for and quantify the Raman scattering.

[13] The analysis of the global group scan is done by an iterative least squares fitting procedure using the following set of 45 equations (i = 1 to 45):

$$\log(I_{oi}/I_i) = A_g + B\frac{(\lambda_i - 315\ \text{nm})}{315\ \text{nm}} + C\Delta\frac{\log(I_{oi})}{\Delta\text{ms}} + D\alpha_i + E\frac{\Delta\alpha_i}{\Delta T} + F\alpha'_i + G\rho_i + \varepsilon_i, \quad (2)$$

where G is the amount of Ring effect apparent in the global scan; ρ_i is the Ring effect vector (Figure 1).

[14] There are three main differences between the global group-scan technique (based on equation (2)) and the direct group-scan techniques (based on equation (1)). The first difference is the exclusion of the Rayleigh scattering term (β_im), which can be calculated for direct irradiance, but becomes part of the offset terms (A_g) and linear term (B) for global irradiance. The second difference is the inability to determine the optical depth of aerosols or thin clouds with the global analysis. Aerosol or cloud optical depth at 315 nm and the Angstrom wavelength exponent [*Angstrom*, 1929] are fairly simply determined from the A_g and B terms of the direct spectra (equation (1)), however, determination of these variables is much more complicated in the case of global irradiance. The third difference is the inclusion of the Ring effect term (G) for global irradiance scans. Thus, for global irradiance analysis there are 15 unknown values (9A_gs, B, C, D, E, F, G) solved by multilinear least squares fit that minimizes the RMS of ε_i, whereas, there are 14 unknown values for the direct irradiance analysis.

[15] The physical meanings of the first 14 unknown values for global irradiance are not necessarily the same as those for direct irradiance. The 9 A_g values are the offsets for the nine groups and account for atmospheric variability (clouds or aerosols) from the entire sky (global) and not just along the direct path (direct). The magnitude of a linear wavelength dependence is the value of B. For global irradiance, the amounts of ozone absorption (D) and SO2 absorption (F) quantify the amount of absorption encountered along a complicated path involving both direct as well as diffuse radiation. However, the wavelength shift (in ms) is the value of C and the effective temperature of ozone is the value of E/D for both global and direct irradiance.

3. Results

[16] For the period between April 2000 and March 2006, there were 44189 group scans made using global irradiance and of these scans 26257 (59%) were "successful." A scan was rejected if the RMS residual was greater than 0.01 (27% of the cases), if the standard deviation of A_g values (indicator of atmospheric variability) was greater than 0.02 (12%), or if the wavelength departure was greater than 16-micrometer steps (2%). The majority of cases with residual greater than 0.01 occurred when the solar zenith angle was greater than 75° with low radiation levels, particularly at shorter wavelengths.

[17] One important parameter determined from the DOAS technique is the shift in wavelength using the solar spectrum as a reference (C in equations (1) and (2)). The wavelength shift using the solar spectrum measures the accuracy of the instrument wavelength calibration and corrects for any offset. Figure 2 shows the record of wavelength shift (in ms; 1 ms ~.007 nm) between 2000 and 2006. The dots are the results for global scans, and the crosses are for the direct scans. In general, there is good agreement between the direct and global results (within ±1 or 2 ms).

[18] Operational wavelength calibrations are carried out using the group of mercury emission lines near 302.1 nm as a reference. The variations with time for both direct and global data shown in Figure 2 provide an indication of the precision of the operational wavelength setting for this particular instrument. Results of the group scan use the solar spectrum as a reference, which is more stable than the

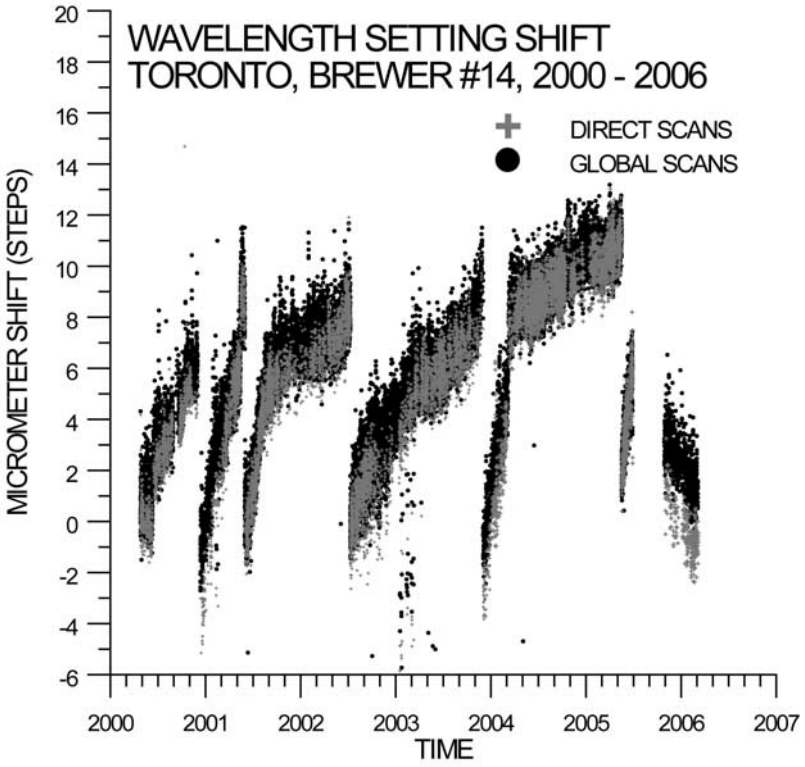

Figure 2. Record of the wavelength shift derived from both direct and global scans for the period April 2000 to March 2006. The wavelength shift is given in micrometer steps and is relative to the extraterrestrial (ET) spectrum measured at Mauna Loa Observatory in March 2000.

output of the mercury lamp. Likely causes for the variations in wavelength calibration include fluctuations in the relative intensity of the mercury lines that occur with temperature or the age of lamp. The sudden jumps in the record occur at times when an old mercury lamp is replaced with a new one. With detailed knowledge of the reference solar spectrum and features in ozone and SO_2 absorption spectra, the effects of wavelength shifts from the reference, as shown in Figure 2, can be accurately corrected [*Kerr*, 2002].

[19] Ozone temperature is one of the atmospheric variables that are determined from the direct and global group-scan data (E/D in equations (1) and (2)). Figure 3 shows the records of effective ozone temperature for the direct and global scan results. The effective ozone temperature is basically the same for both direct and global data and shows the same annual variation. For 9889 near simultaneous direct/global scans the temperature derived from global scans is on average 0.2°C higher than that for the direct scans and the standard deviation of the differences is 1.9°C. The number of global scans successfully analysed (low residuals) is more than twice that for the direct scans. This is because global data are successfully analyzed during cloudy conditions when direct data are not available.

[20] As mentioned earlier, the physical meaning of the ozone absorption term for direct scans (D in equation (1); hereinafter denoted as D_{direct}) is relatively simple and is equal to μX [*Kerr*, 2002]. However, the physical meaning of D in equation (2) for the global scans (D_{global}) is not as simple since global irradiance is composed of direct and diffuse radiation that follows a complicated path through the atmospheric ozone. The relationship between the global and direct ozone absorption terms is shown in Figure 4. Here the ratio of D_{global}/D_{direct} (=R) is plotted as a function of μ for the period from 2000 to 2006. The solid line plotted through the points is a quadratic least squares fit with the formula $R = 1.0780 + 0.00949\ \mu - 0.01791\ \mu^2$. Since total ozone (X) is D_{direct}/μ, it follows that total ozone can be derived from the D_{global} by the relationship

$$X = D_{global}/\left(\mu\left(1.0780 + .00949\ \mu - 0.01791\ \mu^2\right)\right). \quad (3)$$

[21] The RMS scatter of the data points about the quadratic fit is ±0.0093, indicating that the agreement between ozone derived from direct scans and that derived from global scans is ±0.93%. There were no rejected data points and the low scatter (<1%) was observed under all conditions when the direct aerosol/cloud optical depth was measured to be less than 2.0 at 315 nm. This includes many instances when scattered or broken clouds were present.

[22] At smaller μ values ($\mu < 2$), the amount of ozone absorption seen in the global (direct plus diffuse) irradiance is somewhat larger than that seen in the direct irradiance. This is because the effective path length of diffuse irradiance through atmospheric ozone is larger than the direct path length. For example, at $\mu = 1.0$, diffuse radiation reaching the surface integrated over the hemispherical sky must have an effective path length through the atmosphere that is larger than the direct, which passes vertically

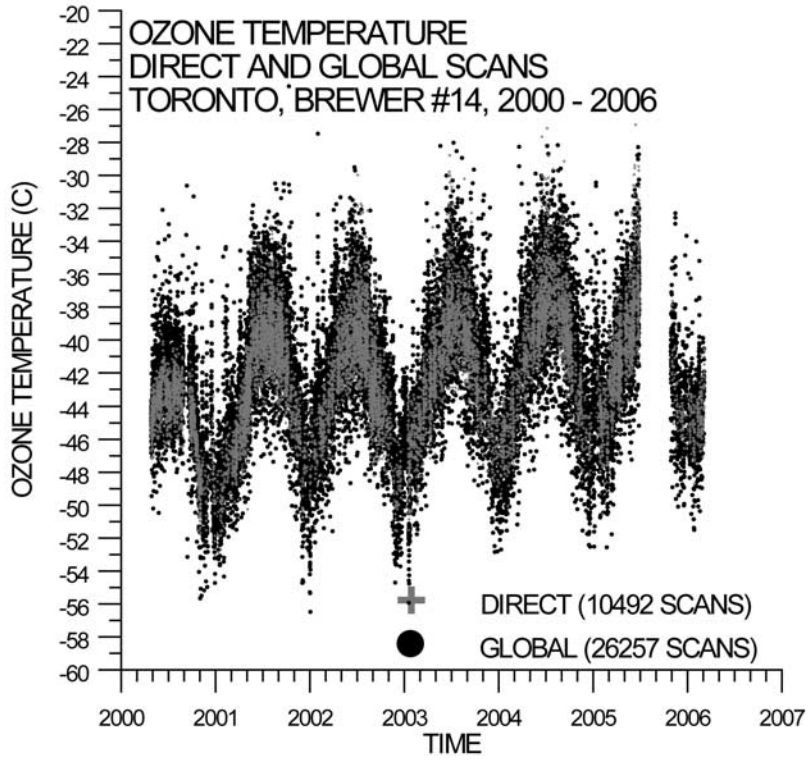

Figure 3. Record of the effective temperature of atmospheric ozone over Toronto for the period derived from both direct and global scans.

downward. However, at a larger μ value (e.g., $\mu \sim 2.4$), the amount of ozone seen in the global irradiance is approximately the same as that seen in the direct irradiance, implying that the effective path length of diffuse irradiance through atmospheric ozone is the same as the direct path.

[23] These results are compared with model results for clear-sky conditions with a standard ozone profile scaled to values 250 DU and 500 DU. The Tropospheric Ultra Violet (TUV) radiative transfer model of *Madronich* [1993] provided the results presented in this study. The model in its standard form allows the user to select the total column ozone. The model provides for the user to specify cloud and aerosol optical properties. In the standard case, the aerosol profile attributed to *Elterman* [1968] is utilized, which

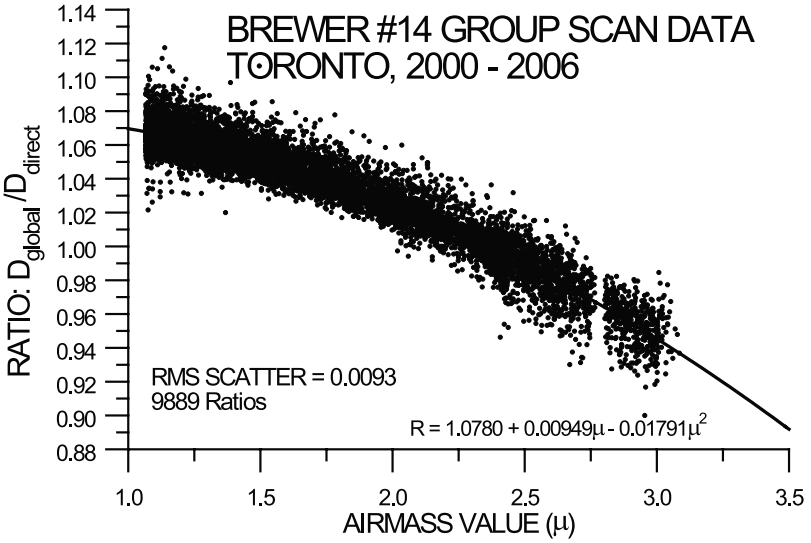

Figure 4. The ratio of ozone derived from global to that of direct scans over the 6-a period. Ozone derived from direct scans is equal to the air mass multiplied by total ozone (μX). It follows that total ozone can be determined from the global scans using the indicated quadratic best fit [i.e., $X = D_{global}/(\mu(1.0780 + .00949\ \mu - 0.01791\ \mu^2))$] with an accuracy of better than 1%.

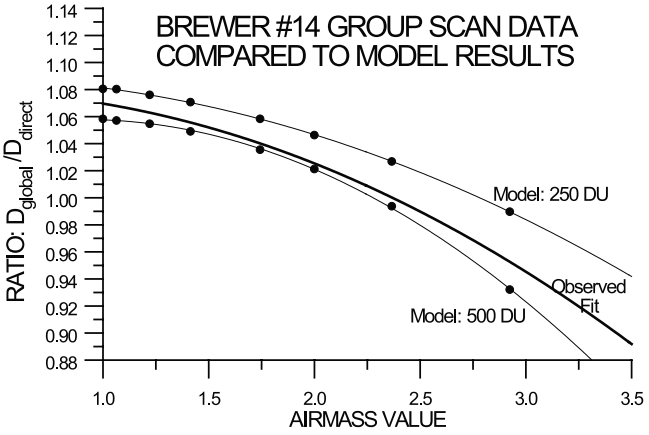

Figure 5. Comparison of the observed best quadratic fit shown in Figure 4 with clear-sky radiative transfer model results for total ozone values of 250 Dobson units (DU) and 500 DU.

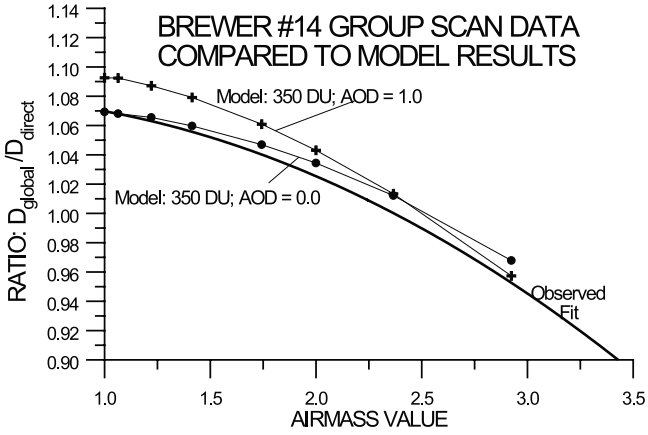

Figure 7. Radiative transfer results indicating that aerosols increase the ozone amount derived from global scans, particularly at smaller air masses.

defines the aerosol optical properties at 340 nm. For the calculations presented in this research, the aerosol optical depths are scaled by an inverse wavelength relationship with the Angstrom wavelength exponent equal to one and the optical depth is specified at 315 nm. This wavelength is used to allow comparison with AOD measurements, which are specified at 315 nm both in this paper as well as that of *Kerr* [2002]. The aerosol single scattering albedo was set at values of 0.85 and 1.0, and the aerosol asymmetry parameter was set at 0.66 at all wavelengths.

[24] The model was run at wavelengths of 305 nm, 310 nm, 315 nm, 320 nm, and 325 nm using ozone absorption coefficients of *Bass and Paur* [1985]. A simple DOAS best fit was carried out on the model results using only an offset term (A), a linear wavelength dependence term (B), and an ozone absorption term (D) as independent variables. The apparent amount of ozone (D) was determined for both direct and global irradiance. Figure 5 shows the comparison of the model results with the fitted average for the 6-a data set. In general, the observations and model results show reasonably good comparability.

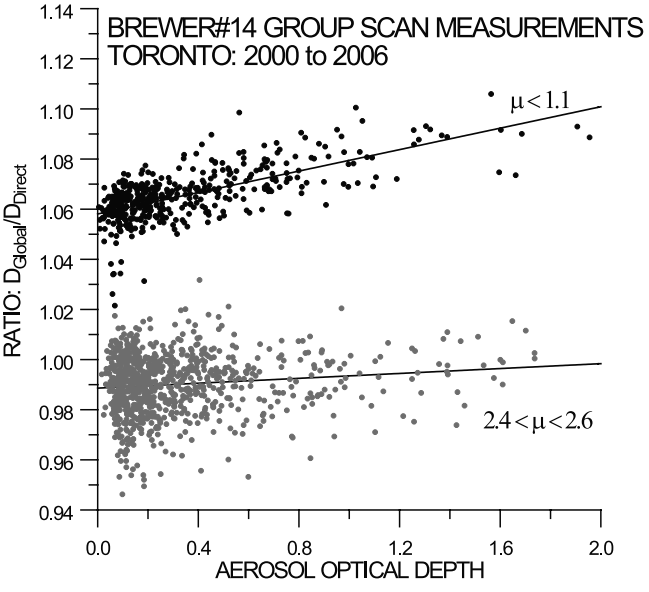

Figure 6. The effect of aerosols on the amount of ozone retrieved from global scans. The aerosol optical depth is from the direct measurements and is valid at 315 nm. In general, the amount of ozone increases with increasing aerosols and is more pronounced at smaller air masses. This is because scattering by aerosols increases the optical path of diffuse radiation through atmospheric ozone.

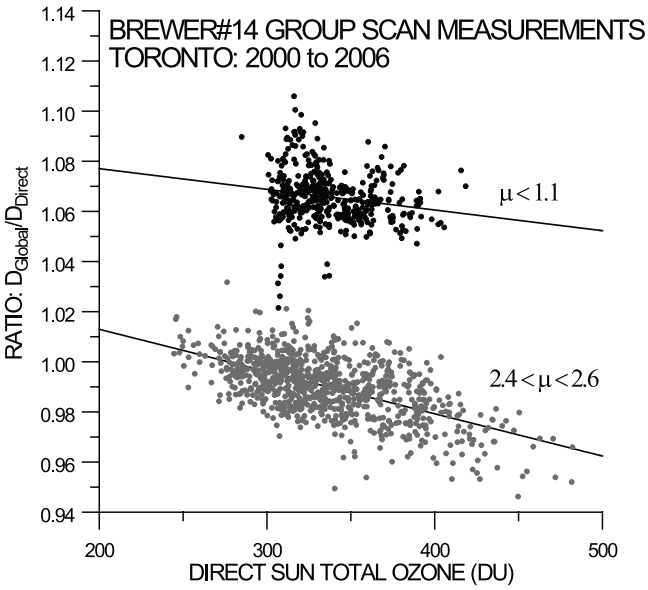

Figure 8. The effect of total ozone on the apparent amount of ozone retrieved from global scans. The apparent amount of ozone decreases with increasing total ozone. This is because ozone absorption of global irradiance is not linear, since the path length through atmospheric ozone decreases with increasing ozone absorption.

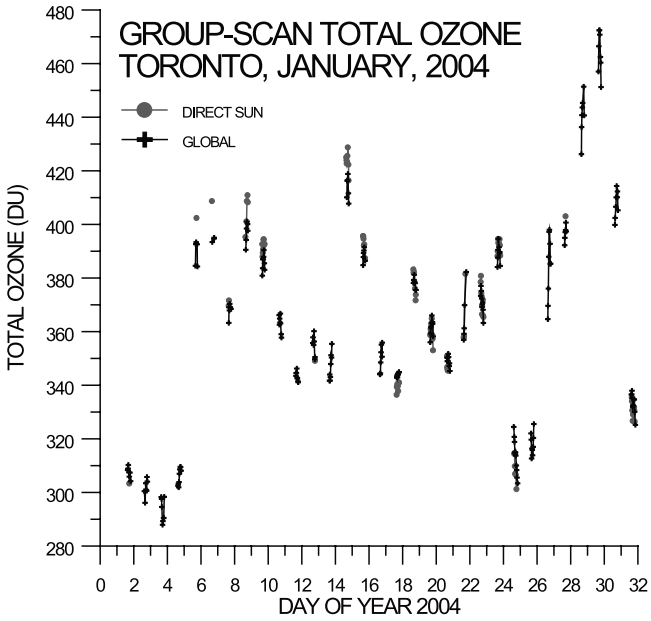

Figure 9. Total ozone derived from global scan data compared with that from direct data for January 2004. There is generally very good agreement between direct and global even at times when the direct Sun is not available.

[25] Figure 6 shows results that summarize the effects of aerosols on global irradiance. Here the value of R is shown as a function of AOD (at 315 nm from direct group-scan measurements) for two air mass ranges ($\mu < 1.1$ and $2.4 < \mu < 2.6$). It is evident that the apparent ozone in global irradiance increases with aerosol optical depth. For an increase of 1.0 in AOD, the enhancement is 2.1% at $\mu \sim 1.1$ and 0.5% at $\mu \sim 2.5$. Figure 7 shows model calculations with 350 DU that compares a clear atmosphere (AOD = 0.0) with one of AOD = 1.0. The calculated results showed little difference between SSA set to 1.0 and SSA at 0.85. The enhanced ozone at $\mu \sim 1.1$ is about 2%, and the enhancement at $\mu \sim 2.5$ is nearly 0, in reasonably good agreement with observations shown in Figure 6.

[26] Figure 8 shows that different total ozone values have an effect on the apparent amount of ozone seen in global irradiance. Here the value of R is plotted as a function of direct Sun total ozone for the air mass ranges of $\mu < 1.1$ and $2.4 < \mu < 2.6$. The slopes of linear fits to these data are -0.000082 for $\mu < 1.1$ and -0.000140 for $2.4 \langle \mu \rangle 2.6$. These dependencies are in reasonably good agreement with model results of Figure 5 which shows decreases of -0.000096 at $\mu = 1$ and -0.000160 at $\mu = 2.5$. The fact that the apparent amount of ozone decreases with an increase of total ozone indicates that the ozone absorption for global irradiance is not quite linear as assumed in the group-scan analysis (equation (2)). This nonlinear absorption will be discussed further later in this paper.

[27] Equation (3) was used to determine total ozone from all global data (26257 scans) for the period. Examples of these total ozone results are shown for two periods in 2004: 1–31 January (Figure 9) and 8 July to 6 August (Figure 10). In general, there is good agreement between the direct and global total ozone retrievals during the winter. All data in Figure 9 were measured when the μ values are greater than 2. However, in summer months (Figure 10), when the Sun is significantly higher in the sky, there can be substantial departures between the direct and global ozone values. These occur on partly cloudy days. There is generally good agreement when direct measurements are possible. However, when the Sun is obscured by cloud, global total ozone values are typically enhanced, particularly when the Sun is high ($\mu < 1.5$).

4. Discussion

[28] As discussed earlier, the measurements and model results indicate that the global radiation absorbed by ozone is slightly nonlinear. There are two causes for the nonlinear absorption. The first is a result of nonuniform absorption across the wavelength band passes of the instrument. This nonlinearity has been thoroughly discussed [*Vanier and Wardle*, 1969; *Gröbner and Kerr*, 2001; *Kerr*, 2002] and is corrected in this work. The second cause for the nonlinear ozone absorption arises from the fact that global irradiance follows a complicated path through atmospheric ozone. The path length depends significantly on the amount and vertical distribution of ozone. Radiation at wavelengths with relatively large ozone absorption is forced to follow a shorter path length through the ozone than radiation with less ozone absorption.

[29] It was observed that the ozone absorption measured in global irradiance is enhanced by atmospheric aerosols and clouds, particularly when the Sun is high ($\mu < 2$). At $\mu \sim 1$ the reason for the enhanced ozone absorption with increasing

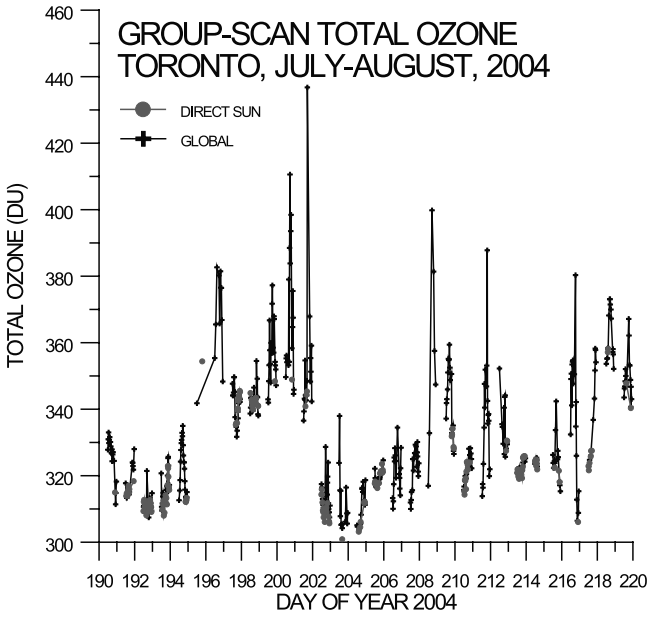

Figure 10. The same as Figure 9 but for summer months (July–August 2004). Here there are often substantial enhancements (~25%) in global total ozone when the Sun is not available. This is likely because of enhanced multiple scattering within convective summertime clouds containing ozone.

aerosol or cloud optical depth is twofold. First, an increase of particulate scattering causes the ratio of diffuse irradiance (with more ozone absorption) to direct irradiance (with less ozone absorption) to increase, thus increasing the amount of apparent ozone absorption. In this case, scattered photons have a longer path length through layers that do not contain clouds or aerosols, but do contain ozone. The second reason for enhanced absorption is that scattering by an aerosol or cloud layer increases the optical path length of global irradiance through atmospheric ozone within the layer [*Fioletov et al.*, 1997]. However, at larger μ values (μ = 2.4), the main reason for enhanced absorption is from scattering within the aerosol or cloud layer since the amount of ozone seen in the direct irradiance is approximately the same as that seen in diffuse irradiance (i.e., R = 1 ± 0.01), as demonstrated in Figure 4.

[30] The scatter of data points in Figure 4 (thereby the accuracy of global total ozone measurement) can be improved if the nonlinearity of ozone absorption and the influence of aerosols are taken into consideration. If nonlinear ozone absorption is included as an independent variable, then the scatter in Figure 4 is reduced marginally to 0.0085 from 0.0093. If AOD is included, the scatter is reduced to 0.0076. The nonlinear absorption can be included as part of the global total ozone reduction (equation (3)). However, the inclusion of the AOD requires information measured by direct Sun scans.

[31] The measurement of total ozone from global irradiance data is a useful product of global UV measurements. Measurements can be made without instrumental pointing requirements and without the presence of direct irradiance. Also, the extension of direct Sun measurement could be made to lower Sun angles. This work has demonstrated a significant improvement of the measurement of total ozone using only global irradiance data. For example, *Fioletov et al.* [1997] quote an uncertainty of about ±6% for total ozone measured from global irradiance data using conventional scanning methods with Brewer instruments, and *Dahlback et al.* [2005] report uncertainties of ±1.4% and ±1.9% respectively for the GUV (ground-based UV) and NILU-UV (Norwegian Institute for Air Research UV) multifilter radiometers. One of the key considerations is the requirement that measurements at several wavelengths in the UV be made simultaneously. The group-scan sampling and analysis technique results in an essentially simultaneous scan measurement. Future plans include the investigation of retrieval from simultaneously sampled global irradiance data measured by other instruments such as the UV-MFRSR.

[32] **Acknowledgments.** James B. Kerr is Scientist Emeritus at Environment Canada. David Wardle, Tom McElroy, and Volodya Savastiouk made valuable suggestions regarding the scientific aspects of the paper. Tom Grajnar provided technical support for the maintenance, calibration, and operation of the instrument. Two anonymous reviewers made constructive suggestions. The U.S. Department of Agriculture's Cooperative State Research, Education, and Extension Service (CSREES) provided funding for this work under contract 2006-34263-16926.

References

Angstrom, A. (1929), On the atmospheric transmission of Sun radiation and on dust in the air, *Geogr. Ann.*, *12*, 130–159.

Bass, A. M., and R. J. Paur (1985), The ultraviolet cross-sections of ozone, I, The measurements, in *Atmospheric Ozone: Proceedings of the Quadrennial Ozone Symposium Held in Halkidiki, Greece, 3–7 September, 1984*, edited by C. S. Zerefos and A. Ghazi, pp. 606–610, D. Reidel, Norwell, Mass.

Bigelow, D. S., and J. R. Slusser (2000), Establishing the stability of multifilter UV rotating shadow-band radiometers, *J. Geophys. Res.*, *105*, 4833–4840.

Booth, C. R., T. B. Lucas, J. H. Morrow, C. S. Weiler, and P. A. Penhale (1994), The United States National Science Foundation/Antarctic program's network for monitoring ultraviolet radiation, in *Ultraviolet Radiation in Antarctica: Measurements and Biological Research*, *Antarct. Res. Ser.*, vol. 62, edited by C. S. Weiler and P. A. Penhale, pp. 17–37, AGU, Washington, D. C.

Dahlback, A. (1996), Measurements of biologically effective UV doses, total ozone abundances, and cloud effects with multichannel, moderate bandwidth filter instruments, *Appl. Opt.*, *35*, 6514–6521.

Dahlback, A., H. A. Eide, B. A. K. Høiskar, R. O. Olsen, F. J. Schmidlin, S.-C. Tsay, and K. Stamnes (2005), Comparison of data for ozone amounts and ultraviolet doses obtained from simultaneous measurements with various standard ultraviolet instruments, *Opt. Eng.*, *44*, 041010-1–041010-9.

Dobson, G. M. B. (1957), Observers' handbook for the ozone spectrophotometer, in *Annual International Geophysical Year*, vol. 5, part 1, pp. 46–89, Pergamon, London.

Elterman, L. (1968), UV, visible, and IR attenuation for altitudes up to 50 km, *AFCRL-68-0153*, Air Force Cambridge Res. Lab., Bedford, Mass.

Fioletov, V. E., J. B. Kerr, and D. I. Wardle (1997), The relationship between total ozone and spectral UV irradiance from Brewer observations and its use for derivation of total ozone from UV measurements, *Geophys. Res. Lett.*, *24*(23), 2997–3000.

Fioletov, V. E., J. B. Kerr, C. T. McElroy, D. I. Wardle, V. Savastiouk, and T. S. Grajnar (2005), The Brewer reference triad, *Geophys. Res. Lett.*, *32*, L20805, doi:10.1029/2005GL024244.

Gao, W., J. Slusser, J. Gibson, G. Scott, D. Bigelow, J. Kerr, and B. McArthur (2001), Direct- sun column ozone retrieval by the ultraviolet multifilter rotating shadow-band radiometer and comparison with those from Brewer and Dobson spectrophotometers, *Appl. Opt.*, *40*, 3149–3155.

Grainger, J. F., and J. Ring (1962), Anomalous Fraunhofer line profiles, *Nature*, *193*, 762.

Gröbner, J., and J. B. Kerr (2001), Ground-based determination of the spectral ultraviolet extraterrestrial solar irradiance: Providing a link between space-based and ground-based solar UV measurements, *J. Geophys. Res.*, *106*, 7211–7217.

Gustin, G. P., et al. (1985), Ozonometer M-124 (in Russian), *Tr. Gl. Geofiz. Obs. Im. A. I. Voeikova*, *499*, 60–67.

Harrison, L., J. Berndt, P. Kriedron, and P. Disterhoft (2002), United States Department of Agriculture reference ultraviolet spectroradiometer: Current performance and operational experience at Table Mountain, Colorado, *Opt. Eng.*, *41*, 3096–3103.

Høiskar, B. A., R. Haugen, T. Danielsen, A. Kylling, K. Edvardsen, A. Dahlback, B. Johnsen, M. Blumthaler, and J. Schreder (2003), Multichannel moderate bandwidth filter instrument for measurement of the ozone column amount, cloud transmission, and ultraviolet dose rates, *Appl. Opt.*, *42*, 3472–3479.

Kerr, J. B. (2002), New methodology for deriving total ozone and other atmospheric variables from Brewer spectrophotometer direct sun spectra, *J. Geophys. Res.*, *107*(D23), 4731, doi:10.1029/2001JD001227.

Kerr, J. B. (2005), Understanding the factors that affect surface ultraviolet radiation, *Opt. Eng.*, *44*, 041002-1–041002-9.

Kerr, J. B., and C. T. McElroy (1993), Evidence for large upward trends of ultraviolet-B radiation linked to ozone depletion, *Science*, *262*, 1032–1034.

Kerr, J. B., C. T. McElroy, and R. A. Olafson (1981), Measurements of ozone with the Brewer spectrophotometer, in *Proceedings of the Quadrennial International Ozone Symposium*, edited by J. London, pp. 74–79, Natl. Cent. for Atmos. Res., Boulder, Colo.

Kiedron, P. W., L. H. Harrison, J. L. Berndt, J. J. Michalsky, and A. F. Beaubien (2001), Specifications and performance of UV rotating shadowband spectroradiometer (UV-RSS), in *Ultraviolet Ground- and Space-based Measurements, Models, and Effects, Proc. SPIE*, *4482*, 249–258.

Langford, A. O., R. Schofield, J. S. Daniel, R. W. Portmann, M. L. Mclamed, H. L. Miller, E. G. Dutton, and S. Solomon (2007), On the variability of the Ring effect in the near ultraviolet: Understanding the role of aerosols and multiple scattering, *Atmos. Chem. Phys.*, *7*, 575–586.

Madronich, S. (1993), UV radiation in the natural and perturbed atmosphere, in *Environmental Effects of Ultraviolet (UV) Radiation*, pp. 17–69, A. F. Lewis, New York.

McElroy, C. T. (1995), A spectroradiometer for the measurement of direct and scattered solar spectral irradiance from on-board the NASA ER-2 high-altitude research aircraft, *Geophys. Res. Lett.*, *22*, 1361–1364.

McKenzie, R. L., W. A. Mathews, and P. V. Johnston (1991), The relationship between erythemal UV and ozone derived from spectral irradiance measurements, *Geophys. Res. Lett.*, *18*, 2269–2272.

Seckmeyer, G., G. Bernhard, B. Mayer, and R. Erb (1996), High accuracy spectroradiometry of solar UV radiation, *Metrologia*, *32*, 697–700.

Vanier, J., and D. I. Wardle (1969), The effects of spectral resolution in total ozone measurements, *Q. J. R. Meteorol. Soc.*, *95*, 395–399.

World Meteorological Organization (2007), Scientific assessment of ozone depletion: 2006, Global ozone research and monitoring project, *Rep. 50*, 748 pp., Geneva.

J. M. Davis, Ultraviolet Radiation Monitoring and Research Program, USDA, 419 Canyon Avenue, Suite 226, Colorado State University, Fort Collins, CO 80523-1499, USA.

J. B. Kerr, Environment Canada, 4396 Kingscote Road, Cowichan Bay, BC, Canada V0R 1N2. (jbkerr@shaw.ca)